

# Ionic self-phoresis maps onto correlation–induced self-phoresis

Alvaro Domínguez<sup>1,2,\*</sup> and Mihail N. Popescu<sup>1,†</sup>

<sup>1</sup>*Física Teórica, Universidad de Sevilla, Apdo. 1065, 41080 Sevilla, Spain*

<sup>2</sup>*Instituto Carlos I de Física Teórica y Computacional, 18071 Granada, Spain*

(Dated: April 26, 2024)

We re-examine the self-phoresis of a particle that releases(removes) pairs of ions into(from) the electrolyte solution. We show analytically that in the linear regime the mathematical description of this system maps onto that of the correlation–induced (self-)chemophoresis (CICP). This connection provides a unifying perspective of the two phenomena, within which one recovers and extends recent predictions as particular instances of CICP. Conversely, ion-phoretic particles are identified as candidates for experimental investigations into the rich variety of motility patterns predicted by CICP.

The emergence of self-motility for chemically active colloidal particles suspended in an aqueous solution of their “fuel” (e.g., hydrogen peroxide for certain bi-metallic rods [1, 2] or platinum-capped dielectric particles [3, 4]) has been the topic of many experimental and theoretical investigations since the first experimental reports were published (insightful reviews of these developments can be found in, e.g., Refs. [5–9]). In many instances, the motility was successfully addressed as self-phoresis (e.g., self-chemophoresis [10–13], self-thermophoresis through a single-component fluid [14], self-chemophoresis via demixing of a critical binary liquid mixture [15–17], or self-electrophoresis [18–22]). That is, motility was interpreted to emerge as a *classic* phoretic linear response to self-generated, rather than externally imposed, non-equilibrium inhomogeneities (in the chemical composition or in the temperature of the solution) [9, 10, 23–25]. Recently, the standard scenario of chemophoresis has been investigated beyond the usual ideal-gas approximation for the solute by accounting for thermodynamic correlations [26, 27]. The result is the identification of a novel mechanism of phoretic motility, the so-called *correlation–induced chemophoresis* (CICP), which provides a paradigm–breaking example that self-phoresis involves in general a non-equilibrium response factor, so that an interpretation as phoresis in self-generated gradients is not possible [26].

In an ubiquitous experimental setup, the particles are charged and the chemical activity consists in the release of ionic radicals in the ambient solution [1, 9, 18, 20, 28–31]. Additionally, there can be electrical currents through the solution and the particle in the case of redox reactions at bi-metallic rods [1, 18], or, as argued by Refs. [21, 22, 32, 33], when a dielectric sphere is covered by a layer of catalyst (a metal or enzymes) of varying thickness.

Recent studies, complementing the earlier works by Refs. [28, 29], have reported a number of interesting features for the case of a spherical particle, such as motility of uncharged particles with non-uniform ionic activity [30] or of non-uniformly charged particles with uniform activity [34]. In particular, in the former case the phoretic velocity was noted to be quadratic in the activ-

ity [30], which evades an interpretation as classic phoresis under self-generated gradients.

Motivated by these insightful observations, here we re-examine a simple model for ionic self-phoresis of a dielectric particle that releases (or removes) pairs of ions in the electrolyte solution. The theoretical analysis is impaired by the nonlinear coupling between the ionic distribution and the electric field [18, 21, 28–30, 34, 35]; accordingly, the use of perturbative expansions has become a standard approach [36–40]. In the linear regime of small surface charge and activity of the particle, we show the unexpected mapping of the mathematical description of this model onto that of the recently reported CICP. On the one hand, this result provides a conceptually clear, unifying perspective which blurs the conceptual distinction between ionic self-phoresis and neutral self-chemophoresis: recent predictions of motility for certain activity and charge patterns then emerge, and are extended, as particular instances of the “selection rules” derived in the CICP model. On the other hand, it highlights ionic self-phoresis as a promising option for experimental investigations into the rich variety of patterns of motility predicted by CICP (see, e.g., the “phase diagram” introduced in Ref. [27]).

*Model system.* – The model we consider consists of a rigid and impermeable dielectric colloidal particle, immersed in a liquid electrolyte solution which is kept at a constant temperature  $T$ . For simplicity, we consider the case of a spherical shape (radius  $R$ ) for the particle, of a symmetric electrolyte (thus two species of ions carrying charges  $\pm q$ ,  $q > 0$ , respectively), and of the dielectric permittivity  $\epsilon$  of the electrolyte solution being much larger than that of the particle. The concentration of the two ionic species are equal to  $c_0 \neq 0$  far from the particle. The particle carries a surface charge  $\sigma_s \mathbb{S}(\mathbf{r}_p)$ , where  $\sigma_s$  is a characteristic value of the surface charge (e.g., its maximum over the surface) and the dimensionless surface field  $\mathbb{S}(\mathbf{r}_p)$ , where  $\mathbf{r}_p$  denotes any point on the surface of the particle, describes the distribution of charge over the surface. The activity of the particle is characterized by the rate per unit surface  $\mathcal{A}\mathbb{A}(\mathbf{r}_p)$  at which pairs of ions are released into ( $\mathbb{A} > 0$ ) or removed from ( $\mathbb{A} < 0$ ) the so-

lution at the position  $\mathbf{r}_p$ ; here,  $\mathcal{A} > 0$  is the maximum absolute value over the surface and the dimensionless surface field  $\mathbb{A}(\mathbf{r}_p)$  describes the pattern of activity [41]. The ions diffuse in the solution with diffusion constants  $D_{\pm}$ ; the associated mobilities are given by the Stokes-Einstein relation as  $\Gamma_{\pm} = \beta D_{\pm}$ , where  $\beta = 1/(k_B T)$ . Finally, the system “particle + electrolyte solution” is assumed to be in mechanical isolation, i.e., there are no external forces or torques acting on either the particle or the fluid: this is the characteristic feature of phoresis which sets it apart from other transport phenomena [23, 42], so that a self-phoretic particle can be actually qualified as a “swimmer”.

When the particle is inactive, the system is in an equilibrium state (fixed by a distant heat bath and reservoirs of ions and solvent), in which the particle and the fluid are motionless. Upon turning on the activity, we assume that a non-equilibrium steady state is established, in which the particle moves and hydrodynamic flow is induced in the electrolyte. Motivated by the observations in typical experimental realizations of active particles, we assume overdamped motion of the particle, while the fluid flow occurs at small Reynolds and Mach numbers (“creeping flow”). Additionally, the particle motion can be assumed slow when compared with the diffusion of the ionic species. Accordingly, the state of the solution is characterized by the instantaneous incompressible flow of the solution and the stationary concentrations  $c_{\pm}(\mathbf{r})$  of each ionic species at small Péclet number (i.e., convection is neglected). An electric field described by a potential  $\psi(\mathbf{r})$  will be also induced due to the local charge imbalances; owing to the assumed large contrast in dielectric constants, the electric field is basically confined to the electrolyte domain.

*Steady-state distribution of ionic species.*— The profiles  $c_{\pm}(\mathbf{r})$  follow from the conservation of ionic species in the bulk expressed in terms of the ion density currents  $\mathbf{j}_{\pm}$ ,

$$\nabla \cdot \mathbf{j}_{\pm} = 0, \quad \mathbf{j}_{\pm} = \Gamma_{\pm} \mathbf{f}_{\pm}. \quad (1)$$

The thermodynamic force densities  $\mathbf{f}_{\pm}$  are determined from the assumption of local equilibrium, consistently with the assumption of slow particle dynamics, as

$$\mathbf{f}_{\pm}(\mathbf{r}) = -c_{\pm}(\mathbf{r}) \nabla \mu_{\pm}(\mathbf{r}), \quad (2)$$

in terms of the local chemical potentials  $\mu_{\pm}(\mathbf{r})$ . The latter are obtained as

$$\mu_{\pm}(\mathbf{r}) = \frac{\delta \mathcal{H}}{\delta c_{\pm}(\mathbf{r})} = \frac{\partial h}{\partial c_{\pm}}(\mathbf{r}) \pm q\psi(\mathbf{r}) \quad (3)$$

from the free energy functional of the electrolyte given by (see, e.g., Refs. [43–45])

$$\begin{aligned} \mathcal{H}[c_+(\mathbf{r}), c_-(\mathbf{r}), \psi(\mathbf{r})] = & \int_{\text{fluid}} d^3 \mathbf{r} \left[ h(c_+, c_-) - \frac{1}{2} \epsilon |\nabla \psi|^2 \right. \\ & \left. + q(c_+ - c_-) \psi - \sigma_s \mathbb{S}(\mathbf{r}_p) \psi \delta(|\mathbf{r}| - R) \right]. \quad (4) \end{aligned}$$

Here,  $\psi(\mathbf{r})$  denotes the electric potential, and  $h(c_+, c_-)$  is a local free energy density that depends implicitly on temperature. A simple and frequently employed choice is the ideal gas form,

$$\beta h(c_+, c_-) = c_+ \left( \ln \frac{c_+}{c_0} - 1 \right) + c_- \left( \ln \frac{c_-}{c_0} - 1 \right). \quad (5)$$

In such case, Eqs. (1), (2), and (3) render the usually employed Nernst–Planck equations. Although the formalism to be presented can be applied in full generality, for instance by addressing a local free energy  $h$  that accounts for steric effects, we will also use Eq. (5) both for reasons of simplicity and for straightforward comparison with previous studies.

The equations are supplemented by the boundary conditions at infinity,

$$\mu_{\pm}(|\mathbf{r}| \rightarrow \infty) \rightarrow \mu_0, \quad c_{\pm}(|\mathbf{r}| \rightarrow \infty) \rightarrow c_0, \quad (6a)$$

and at the surface of the particle, where the catalytic activity is modeled as a current along the direction normal to the particle:

$$\mathbf{e}_r \cdot \mathbf{j}_+(\mathbf{r}_p) = \mathbf{e}_r \cdot \mathbf{j}_-(\mathbf{r}_p) = \mathcal{A} \mathbb{A}(\mathbf{r}_p). \quad (6b)$$

*Electric field.*— The potential  $\psi(\mathbf{r})$  in the fluid is determined from the minimization of the free energy functional with respect to  $\psi(\mathbf{r})$ , i.e., by solving  $\delta \mathcal{H} / \delta \psi(\mathbf{r}) = 0$ . This renders the Poisson equation,

$$\nabla^2 \psi(\mathbf{r}) = -\frac{q}{\epsilon} [c_+(\mathbf{r}) - c_-(\mathbf{r})], \quad (7)$$

and the boundary condition at the surface of the particle,

$$\mathbf{e}_r \cdot \nabla \psi(\mathbf{r}_p) = -\frac{\sigma_s}{\epsilon} \mathbb{S}(\mathbf{r}_p), \quad (8a)$$

associated to a high dielectric constant. These are supplemented by the boundary condition at infinity,

$$\psi(|\mathbf{r}| \rightarrow \infty) \rightarrow 0. \quad (8b)$$

*Hydrodynamics and the motion of the particle.*— The flow is determined by the incompressible Stokes equations, i.e., by the mechanical balance between the fluid stresses and the body force density,  $\mathbf{f}(\mathbf{r}) := \mathbf{f}_+(\mathbf{r}) + \mathbf{f}_-(\mathbf{r})$ , acting on the solution, complemented by boundary conditions at infinity (quiescent fluid) and at the surface of the particle (no slip) [46]. The translational and rotational velocities,  $\mathbf{V}$  and  $\mathbf{\Omega}$  respectively, of the overdamped motion of the particle can be obtained from the condition of mechanical isolation of the composed system “particle+solution” by using the Lorentz reciprocal theorem, without the need to compute first the velocity field in the fluid [11, 19, 26, 47, 48]:

$$\mathbf{V} = \frac{1}{6\pi\eta R} \int_{\text{fluid}} d^3 \mathbf{r} \mathbf{K}(\mathbf{r}) \cdot \mathbf{f}(\mathbf{r}), \quad (9a)$$

$$\mathbf{\Omega} = \frac{1}{8\pi\eta R^3} \int_{\text{fluid}} d^3 \mathbf{r} \mathbf{K}(\mathbf{r}) \times \mathbf{f}(\mathbf{r}), \quad (9b)$$

where the (in general non-symmetric) tensorial kernel  $\mathbf{K}(\mathbf{r})$  and the vectorial kernel  $\mathbf{K}(\mathbf{r})$  are determined solely by the geometrical shape of the particle [49, 50]. These fields incorporate the incompressibility constraint as ( $\mathbf{K}^\dagger$  is the transposed tensor)

$$\nabla \cdot \mathbf{K}^\dagger = 0, \quad \nabla \times \mathbf{K} = 0. \quad (10)$$

This ensures that only the solenoidal component of  $\mathbf{f}$  contributes in Eqs. (9) to the motion of the particle [26, 48]. For the specific case of a spherical particle, they take the form

$$\mathbf{K}(\mathbf{r}) = \left[ \frac{1}{4} \left( \frac{R}{r} \right)^3 + \frac{3R}{4r} - 1 \right] \mathbf{I} + \frac{3R}{4r} \left[ 1 - \left( \frac{R}{r} \right)^2 \right] \mathbf{e}_r \mathbf{e}_r, \quad (11a)$$

$$\mathbf{K}(\mathbf{r}) = \left[ \left( \frac{R}{r} \right)^3 - 1 \right] r \mathbf{e}_r, \quad (11b)$$

in spherical coordinates with origin at the center of the sphere, where  $\mathbf{e}_r$  is the unit radial vector and  $\mathbf{I}$  is the identity tensor.

*Quasi-homogenous regime and mapping to CICP.*— The coupled Eqs. (1) and (7) cannot be solved analytically in general and progress can be made only after approximations. We will focus on the case that the activity of the particle and the surface charge are both very small, so that the system is only weakly out of a spatially homogeneous equilibrium state. Thus, the equations governing the ionic distribution will be solved perturbatively to leading order in the deviations  $\delta c_\pm(\mathbf{r}) := c_\pm(\mathbf{r}) - c_0$  [51]. In this approximation, Eqs. (3-5) lead to

$$\delta \mu_\pm := \mu_\pm - \mu_0 = \frac{1}{\beta c_0} \delta c_\pm \pm q\psi, \quad (12)$$

and one finds that the force density is given by [46]

$$\mathbf{f}(\mathbf{r}) = -\frac{1}{2} Q \nabla M - \frac{1}{4\beta c_0} \nabla N^2 \equiv -\frac{1}{2} Q(\mathbf{r}) \nabla M(\mathbf{r}), \quad (13)$$

in terms of the local charge density (up to a factor  $q$ ),

$$Q(\mathbf{r}) := \delta c_+ - \delta c_- = c_+ - c_-, \quad (14)$$

the local contrast in chemical potential,

$$M(\mathbf{r}) := \delta \mu_+ - \delta \mu_- = \mu_+ - \mu_-, \quad (15)$$

and the total concentration of ions  $N(\mathbf{r}) := \delta c_+ + \delta c_-$ . This latter field has no effect whatsoever on the motility due to Eqs. (10) for the incompressibility constraint, in spite of it varying in space, as it appears in Eq. (13) as an additive gradient that can be dropped. Therefore, only charge imbalances matter in the linear approximation. Upon defining the parameter

$$\frac{1}{\Delta} := \frac{1}{D_+} - \frac{1}{D_-}, \quad (16)$$

and the Debye length

$$\lambda_D := \sqrt{\frac{\epsilon}{2q^2\beta c_0}}, \quad (17)$$

one finds [46] that Eqs. (1) lead to the boundary value problem

$$\nabla^2 M(\mathbf{r}) = 0, \quad (18a)$$

$$\mathbf{e}_r \cdot \nabla M(\mathbf{r}_p) = -\frac{\mathcal{A}}{\beta c_0 \Delta} \mathbb{A}(\mathbf{r}_p), \quad (18b)$$

$$M(|\mathbf{r}| \rightarrow \infty) = 0, \quad (18c)$$

while the electrostatic equation (7) yields the boundary-value problem

$$\nabla^2 Q(\mathbf{r}) = \frac{1}{\lambda_D^2} Q(\mathbf{r}), \quad (19a)$$

$$\mathbf{e}_r \cdot \nabla Q(\mathbf{r}_p) = -\frac{\mathcal{A}}{\Delta} \mathbb{A}(\mathbf{r}_p) + \frac{\sigma_s}{q\lambda_D^2} \mathbb{S}(\mathbf{r}_p), \quad (19b)$$

$$Q(|\mathbf{r}| \rightarrow \infty) = 0. \quad (19c)$$

The equations (13, 18, 19) have the same mathematical structure as the model for self-phoretic motility by CICP [26], with  $\lambda_D$  playing the role of the correlation length [46]. This mathematical mapping, which is the main result of this work, allows one to directly import the results for  $\mathbf{V}, \mathbf{\Omega}$  derived by Ref. [26] to the current problem of ionic self-phoresis. It provides a conceptually clear and physically insightful unifying perspective on a number of previously reported results. A first, immediate result is the absence of phoretic motility in this approximation when the two ionic species have the same diffusivity ( $\Delta^{-1} = 0 \Rightarrow M = 0 \Rightarrow \mathbf{f} = 0$ ) [30, 34].

The solution of Eqs. (19) can be written as the superposition  $Q(\mathbf{r}) = Q^{(\mathbb{A})}(\mathbf{r}) + Q^{(\mathbb{S})}(\mathbf{r})$  [46], where  $Q^{(\mathbb{S})}(\mathbf{r})$  is the charge distribution induced solely by the particle surface charge (i.e., the charge distribution in equilibrium), while  $Q^{(\mathbb{A})}(\mathbf{r})$  is the charge distribution due to activity alone — since  $\mathbb{A}$  enters Eqs. (19) on equal footing with  $\mathbb{S}$ , the activity appears to renormalize the particle's charge. Accordingly, the phoretic velocities are, via Eqs. (9, 13), similarly decomposed. By expanding the activity in spherical harmonics,

$$\mathbb{A}(\mathbf{r}_p) = \sum_{\ell=0}^{\infty} \sum_{m=-\ell}^{\ell} a_{\ell m} Y_{\ell m}(\theta, \varphi), \quad (20)$$

and likewise for the other surface field  $\mathbb{S}(\mathbf{r}_p)$  (with coefficients  $s_{\ell m}$ ), one can write [26, 46]

$$\mathbf{V} = \sum_{\ell m, \ell' m'} \left[ \left( \frac{R}{\lambda_D} \right)^2 V^{(\mathbb{S})} s_{\ell m} - V^{(\mathbb{A})} a_{\ell m} \right] a_{\ell' m'} \quad (21a)$$

$$\times \left[ g_{\ell \ell'}^\perp \left( \frac{\lambda_D}{R} \right) \mathbf{G}_{\ell m; \ell' m'}^\perp + g_{\ell \ell'}^\parallel \left( \frac{\lambda_D}{R} \right) \mathbf{G}_{\ell m; \ell' m'}^\parallel \right],$$

$$\mathbf{\Omega} = \sum_{\ell m, \ell' m'} \left( \frac{R}{\lambda_D} \right)^2 \Omega^{(\mathbb{S})} s_{\ell m} a_{\ell' m'} g_{\ell \ell'}^\tau \left( \frac{\lambda_D}{R} \right) \mathbf{G}_{\ell m; \ell' m'}^\tau \quad (21b)$$

with the characteristic velocity scales

$$V^{(\text{A})} := \frac{q^2 R^5 \mathcal{A}^2}{6\pi\eta\epsilon\Delta^2}, \quad V^{(\text{S})} := \frac{qR^3 \mathcal{A}\sigma_s}{6\pi\eta\epsilon\Delta}, \quad \Omega^{(\text{S})} := \frac{3V^{(\text{S})}}{4R}. \quad (21\text{c})$$

In these expressions, the dimensionless functions  $g^\parallel$ ,  $g^\perp$ ,  $g^\tau$  encode the dependence on the bulk concentration  $c_0$  through the Debye length, and the dimensionless vectors  $\mathbf{G}^\perp$ ,  $\mathbf{G}^\parallel$ ,  $\mathbf{G}^\tau$ , which are purely geometrical factors independent of any system parameters, vanish for certain combinations of modes  $\{\ell, m\}$  and  $\{\ell', m'\}$  — accordingly, they imply “selection rules”, i.e., those modes do not contribute to the phoretic velocities:

$$\left. \begin{array}{l} \mathbf{G}_{\ell m; \ell' m'}^\perp = 0 \\ \mathbf{G}_{\ell m; \ell' m'}^\parallel = 0 \end{array} \right\} \text{ if } \left\{ \begin{array}{l} \ell - \ell' \neq \pm 1, \text{ or} \\ m + m' \neq 0, \pm 1, \end{array} \right. \quad (22\text{a})$$

$$\mathbf{G}_{\ell m; \ell' m'}^\tau = 0 \quad \text{if } \left\{ \begin{array}{l} \ell - \ell' \neq 0, \text{ or} \\ \ell = \ell' = 0, \text{ or} \\ m = m', \text{ or} \\ m + m' \neq 0, \pm 1. \end{array} \right. \quad (22\text{b})$$

The index  $\parallel$  denotes the contributions coming from the components of the force (13) tangential to the surface of the spherical particle, while  $\perp$  pertains to the normal component. The angular velocity  $\Omega$  only receives contributions from the tangential components [26].

*Discussion.* — For the physical interpretation of Eqs. (21), it is useful to separately highlight [27] the *source of phoresis*, associated to the problem (18) describing how the system is driven out of equilibrium (in this case, the only source is activity), and the *mechanisms of phoresis*, associated to the problem (19), which concerns how particle motion emerges.

Pertaining to translation, there are two contributions in  $\mathbf{V}$ , similar in mathematical structure but with different physical meaning and dependence on the system parameters. Thus, the “surface-charge-driven mechanism” corresponding to  $V^{(\text{S})}$  follows from the coupling between the equilibrium charge distribution induced by the particle charge (the piece  $Q^{(\text{S})}(\mathbf{r})$  of the solution to Eqs. (19)), and the departure from equilibrium driven by activity. This component of the motility mechanism can be captured by linear-response theory and may eventually be interpreted as “phoresis in self-generated gradients”. On the contrary, the contribution associated to  $Q^{(\text{A})}(\mathbf{r})$  and  $V^{(\text{A})}$ , which depends entirely on activity and was first identified in Refs. [26, 30], precludes a similar interpretation due to the specific bi-linear dependence on the activity rate  $\mathcal{A}$ ; that is, it cannot be derived in the classic framework of Ref. [36]. This contribution is precisely the “correlation-driven mechanism” of chemophoresis [26, 27], so termed because it vanishes in the absence of correlations (i.e., when  $\lambda_D \rightarrow 0$ , see, c.f., Eqs. (23)).

As for the rotational velocity  $\Omega$ , it highlights the conceptual difference between the two mechanisms, which manifests qualitatively by the lack of a contribution  $\Omega^{(\text{A})}$ .

As shown by Ref. [26], this is due to the fact that chirality is not broken when both the source and the mechanism of phoresis (as defined above) have the same origin — the chemical activity, in this case. On the other hand, in the generic case that the origins are unrelated, as in the case of activity vs. surface charge, a preferred direction of rotation emerges for the particle to attempt to restore equilibrium, which explains the contribution  $\Omega^{(\text{S})}$  that is linear in the activity and in the charge. Accordingly, in experimental studies the rotational phoresis could play a key role in disentangling the contributions of the two mechanisms (surface-charge-driven vs. correlation-driven), as in this quasi-homogeneous approximation  $\Omega$  is the telltale signature of, and it is in whole attributed to, the former.

The selection rules (22) provide constraints on how motility emerges. Focusing on the translational motion, it occurs through the coupling of successive multipoles of source and mechanism, respectively (activity and surface charge for  $V^{(\text{S})}$ , or just activity for  $V^{(\text{A})}$ ). This ensures that at least one of the two is polar, i.e., there must exist a “fore-aft” asymmetry in the particle surface properties. The simplest choices are, e.g., a monopole plus dipole of activity ( $a_{\ell m} = 0$  if  $\ell \geq 2$ ), with either a monopolar surface charge ( $s_{\ell m} = 0$  if  $\ell \neq 0$ ) as was done in Ref. [30], or with a monopole plus dipole of surface charge ( $s_{\ell m} = 0$  if  $\ell \geq 2$ ) as was the case in Ref. [34]. But, obviously, Eqs. (21) allow one to predict very many other choices of activity patterns for which motion would occur, e.g., activity patterns missing the monopolar and dipolar components but possessing a quadrupole component which would couple with the dipole of the surface charge. This observation also clarifies that Ref. [29] missed the “correlation-driven” contribution (quadratic in the activity) not because the particle considered was not a net source of ion pairs ( $a_{00} = 0$ ), but rather because activity was modeled *with a single* multipole.

The phoretic velocities depend on the background ion concentration  $c_0$  through the ratio  $\lambda_D/R$  as encoded by the  $g$  functions. The dependence may be quite complex, but robust features emerge in the limiting cases. When  $\lambda_D/R \rightarrow 0$  (the so-called “thin-(Debye)-layer approximation” [11, 23, 25, 26, 29, 36, 40, 42], because the force field  $\mathbf{f}(\mathbf{r})$  is non-vanishing only in a thin layer lying on the particle surface), one gets the universal behavior [46]

$$g_{\ell\ell'}^\parallel \approx \frac{3}{2} \left( \frac{\lambda_D}{R} \right)^5, \quad g_{\ell\ell'}^\perp \approx 2 \frac{\lambda_D}{R} g_{\ell\ell'}^\parallel, \quad g_{\ell\ell'}^\tau \approx 2g_{\ell\ell'}^\parallel. \quad (23)$$

That is, in this limit the phoretic velocities are dominated by the tangential components of the force and they are predicted to vanish with increasing electrolyte concentration as  $V, \Omega \sim c_0^{-3/2}$  if  $V^{(\text{S})} \neq 0$ , or as  $V \sim c_0^{-5/2}$  if  $V^{(\text{S})} = 0$ . A vanishing velocity agrees [52] with experimental observations [12, 32, 33]. In the opposite limit,  $\lambda_D/R \rightarrow \infty$ , the phoretic velocities  $\mathbf{V}, \Omega$  reach finite values that are independent of  $\lambda_D$  (thus of  $c_0$ ) [46]. It is

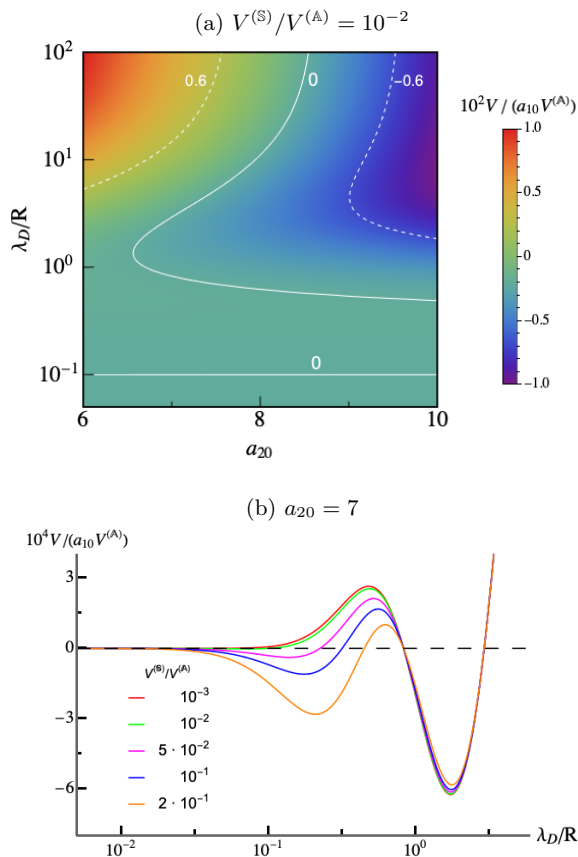


FIG. 1. Translation velocity  $V = \mathbf{e}_z \cdot \mathbf{V}$  as a function of the scaled Debye length  $\lambda_D/R$ , the quadrupolar moment  $a_{20} (\equiv s_{20})$ , and the ratio  $V^{(S)}/V^{(A)}$  (see the main text for details). It is shown in (a) at fixed  $V^{(S)}/V^{(A)} = 10^{-2}$  (white curves are contour lines of constant  $V$ ) and in (b) at fixed  $a_{20} = s_{20} = 7$ .

noteworthy that both limiting behaviors hold regardless of the specific combination of activity and surface charge multipoles, and thus extend the results reported for specific choices [28–30, 34].

Beyond these limiting cases, the different dependence on the system parameters of the two contributions to  $\mathbf{V}$ , but also the combination of multipole moments in each of them, can be expected to lead generically to changes in the direction of motion upon varying  $c_0$  and  $R$  [29, 30, 34], even multiple times [26]. Figure 1 provides an illustrative example of the complexity emerging when going beyond the usually considered configuration of monopole plus dipole; e.g., we consider a model system with  $a_{00} = s_{00} = 1$ ,  $a_{10} = s_{10} \neq 0$ ,  $a_{20} = s_{20} \neq 0$ , all other multipoles being zero [53], so that  $\mathbf{V} = \mathbf{e}_z V$ ,  $\mathbf{\Omega} = 0$  according to Eqs. (21), and choose realistic values of the ratio  $V^{(S)}/V^{(A)} = \sigma_s \Delta / q R^2 \mathcal{A}$  [54]. Panel (a) shows that, upon varying the Debye length, the translational velocity can change sign once (e.g., at  $a_{20} = 6$ ), twice (at  $a_{20} \approx 6.5$ ), or three times (e.g., at  $a_{20} = 7$ )

due to the competition between the two mechanisms in Eq. (21a) (surface-charge-driven vs. correlation-driven). In panel (b) we illustrate how this behavior depends on the ratio  $V^{(S)}/V^{(A)}$  for a fixed  $a_{20} = 7$ . Moreover, it highlights that the values of the Debye length where this competition is more significant lies in the experimentally accessible range (from  $R = 1 \mu\text{m}$  and  $\lambda_D/R = 10^{-2}$ , corresponding to  $\sim 1 \text{ mM}$  salt concentration, to  $R = 100 \text{ nm}$  and  $\lambda_D/R = 3$  for deionized water). This behavior bears similarity with certain experimental observations, both in self-phoresis [55] and in classical phoresis in electrolyte gradients [39].

*Conclusion.*— We have shown that an exact mathematical mapping exists between a model of ionic self-phoresis and the model of correlation-induced self-phoresis introduced in Ref. [26]. This conceptual connection builds a consistent unifying perspective for previously derived results, provides several additional theoretical predictions, and reveals insightful similarities between ionic self-phoresis and self-chemophoresis.

A number of directions for further exploration emerge. A study beyond the quasi-homogeneous approximation, e.g., layering effects due to a finite ion size, should reveal to what extent the mapping holds beyond this simplification. An extension to the case of multiple types of ion pairs in the electrolyte, including electrolytes with asymmetric ions, would be also useful in order to address realistic experimental configurations. Finally, it would be interesting to examine other mechanisms of ionic activity that involve either the release of a single species of ions, e.g., the redox reactions in bi-metallic structures [18], or an ion exchange with the electrolyte, as in the case of the Nafion [57, 58] or resin [59, 60] particles.

The authors acknowledge financial support through grants ProyExcel.00505 funded by Junta de Andalucía, and PID2021-126348NB-I00 funded by MCIN/AEI/10.13039/501100011033 and “ERDF A way of making Europe”. M.N.P. also acknowledges support from Ministerio de Universidades through a María Zambrano grant.

\* [dominguez@us.es](mailto:dominguez@us.es)

† [mpopescu@us.es](mailto:mpopescu@us.es)

- [1] W. F. Paxton, K. C. Kistler, C. C. Olmeda, A. Sen, S. K. St. Angelo, Y. Y. Cao, T. E. Mallouk, P. E. Lammert, and V. H. Crespi, Catalytic nanomotors: Autonomous movement of striped nanorods, *J. Am. Chem. Soc.* **126**, 13424 (2004).
- [2] S. Fournier-Bidoz, A. C. Arsenault, I. Manners, and G. A. Ozin, Synthetic self-propelled nanorotors, *Chem. Commun.*, 441 (2005).
- [3] J. R. Howse, R. A. L. Jones, A. J. Ryan, T. Gough, R. Vafabakhsh, and R. Golestanian, Self-motile colloidal particles: From directed propulsion to random walk, *Phys. Rev. Lett.* **99**, 048102 (2007).

- [4] L. Baraban, M. Tasinkevych, M. N. Popescu, S. Sánchez, S. Dietrich, and O. Schmidt, Transport of cargo by catalytic Janus micro-motors, *Soft Matter* **8**, 48 (2012).
- [5] S. J. Ebbens and J. R. Howse, In pursuit of propulsion at the nanoscale, *Soft Matter* **6**, 726 (2010).
- [6] C. Bechinger, R. Di Leonardo, H. Löwen, C. Reichhardt, G. Volpe, and G. Volpe, Active particles in complex and crowded environments, *Rev. Mod. Phys.* **88**, 045006 (2016).
- [7] K. K. Dey, F. Wong, A. Altemose, and A. Sen, Catalytic motors—Quo Vadimus?, *Curr. Op. Colloid Interf. Sci.* **21**, 4 (2016).
- [8] A. Aubret, S. Ramanarivo, and J. Palacci, Eppur si muove, and yet it moves: Patchy (phoretic) swimmers, *Curr. Op. Colloid Interf. Sci.* **30**, 81 (2017).
- [9] J. L. Moran and J. D. Posner, Phoretic self-propulsion, *Annu. Rev. Fluid Mech.* **49**, 511 (2017).
- [10] R. Golestanian, T. B. Liverpool, and A. Ajdari, Propulsion of a molecular machine by asymmetric distribution of reaction products, *Phys. Rev. Lett.* **94**, 220801 (2005).
- [11] N. Sharifi-Mood, J. Koplik, and C. Maldarelli, Diffusiophoretic self-propulsion of colloids driven by a surface reaction: The sub-micron particle regime for exponential and van der Waals interactions, *Phys. Fluids* **25**, 012001 (2013).
- [12] J. Palacci, S. Sacanna, A. P. Steinberg, D. J. Pine, and P. M. Chaikin, Living crystals of light-activated colloidal surfers, *Science* **339**, 936 (2013).
- [13] J. Simmchen, J. Katuri, W. E. Uspal, M. N. Popescu, M. Tasinkevych, and S. Sánchez, Topographical pathways guide chemical microswimmers, *Nat. Comm.* **7**, 10598 (2016).
- [14] K. Kroy, D. Chakraborty, and F. Cichos, Hot microswimmers, *Eur. Phys. J. Spec. Topics* **225**, 2207 (2016).
- [15] G. Volpe, I. Buttinoni, D. Vogt, H.-J. Kümmerer, and C. Bechinger, Microswimmers in patterned environments, *Soft Matter* **7**, 8810 (2011).
- [16] A. Würger, Self-diffusiophoresis of Janus particles in near-critical mixtures, *Phys. Rev. Lett.* **115**, 188304 (2015).
- [17] S. Samin and R. van Roij, Self-propulsion mechanism of active Janus particles in near-critical binary mixtures, *Phys. Rev. Lett.* **115**, 188305 (2015).
- [18] J. L. Moran and J. D. Posner, Electrokinetic locomotion due to reaction-induced charge auto-electrophoresis, *J. Fluid Mech.* **680**, 31 (2011).
- [19] B. Sabass and U. Seifert, Dynamics and efficiency of a self-propelled, diffusiophoretic swimmer, *J. Chem. Phys.* **136**, 064508 (2012).
- [20] C. Liu, C. Zhou, W. Wang, and H. P. Zhang, Bimetallic microswimmers speed up in confining channels, *Phys. Rev. Lett.* **117**, 198001 (2016).
- [21] Y. Ibrahim, R. Golestanian, and T. B. Liverpool, Multiple phoretic mechanisms in the self-propulsion of a Pt-insulator Janus swimmer, *J. Fluid Mech.* **828**, 318 (2017).
- [22] M. Allan, A. Brooks, M. Tasinkevych, S. Sabrina, D. Velegol, A. Sen, and K. Bishop, Shape-directed rotation of homogeneous micromotors via catalytic self-electrophoresis, *Nature Commun.* **10**, 495 (2019).
- [23] J. L. Anderson, Colloid transport by interfacial forces, *Annu. Rev. Fluid Mech.* **21**, 61 (1989).
- [24] G. Ruckner and R. Kapral, Chemically powered nanodimers, *Phys. Rev. Lett.* **98**, 150603 (2007).
- [25] S. Michelin and E. Lauga, Phoretic self-propulsion at finite Péclet numbers, *J. Fluid Mech.* **747**, 572 (2014).
- [26] A. Domínguez, M. N. Popescu, C. M. Rohwer, and S. Dietrich, Self-motility of an active particle induced by correlations in the surrounding solution, *Phys. Rev. Lett.* **125**, 268002 (2020).
- [27] A. Domínguez and M. N. Popescu, A fresh view on phoresis and self-phoresis, *Curr. Op. Colloid Interf. Sci.* **61**, 101610 (2022).
- [28] P. Bayati and A. Najafi, Dynamics of two interacting active Janus particles, *J. Chem. Phys.* **144**, 134901 (2016).
- [29] A. T. Brown, W. C. K. Poon, C. Holm, and J. de Graaf, Ionic screening and dissociation are crucial for understanding chemical self-propulsion in polar solvents, *Soft Matter* **13**, 1200 (2017).
- [30] M. De Corato, X. Arqué, T. Patiño, M. Arroyo, S. Sánchez, and I. Pagonabarraga, Self-propulsion of active colloids via ion release: Theory and experiments, *Phys. Rev. Lett.* **124**, 108001 (2020).
- [31] E. S. Asmolov, T. V. Nizkaya, and O. I. Vinogradova, Self-diffusiophoresis of Janus particles that release ions, *Physics of Fluids* **34**, 032011 (2022).
- [32] S. Ebbens, D. A. Gregory, G. Dunderdale, J. R. Howse, Y. Ibrahim, T. B. Liverpool, and R. Golestanian, Electrokinetic effects in catalytic platinum-insulator Janus swimmers, *EPL* **106**, 58003 (2014).
- [33] A. Brown and W. Poon, Ionic effects in self-propelled Pt-coated Janus swimmers, *Soft Matter* **10**, 4016 (2014).
- [34] A. Shrestha and M. Olvera de la Cruz, Enhanced phoretic self-propulsion of active colloids through surface charge asymmetry, *Phys. Rev. E* **109**, 014613 (2024).
- [35] T. Nizkaya, E. Asmolov, and O. Vinogradova, Theoretical modeling of catalytic self-propulsion, *Curr. Op. Colloid Interf. Sci.* **62**, 101637 (2022).
- [36] D. C. Prieve, J. L. Anderson, J. P. Ebel, and M. E. Lowell, Motion of a particle generated by chemical gradients. Part 2. Electrolytes, *J. Fluid Mech.* **148**, 247 (1984).
- [37] J. L. Anderson and D. C. Prieve, Diffusiophoresis: Migration of colloidal particles in gradients of solute concentration, *Sep. Purif. Meth.* **13**, 67 (1984).
- [38] D. C. Prieve and R. Roman, Diffusiophoresis of a rigid sphere through a viscous electrolyte solution, *J. Chem. Soc., Faraday Trans. 2* **83**, 1287 (1987).
- [39] J. P. Ebel, J. L. Anderson, and D. C. Prieve, Diffusiophoresis of latex particles in electrolyte gradients, *Langmuir* **4**, 396 (1988).
- [40] S. Dukhin, Non-equilibrium electric surface phenomena, *Adv. Colloid Interf. Sci.* **44**, 1 (1993).
- [41] We have chosen the case that the ions taking part in the catalytic reaction are of the same species as the ones already present in the background electrolyte for reasons of conceptual simplicity. The study can be straightforwardly extended to the case of different ion pairs, but at the expense of significantly more cumbersome algebra.
- [42] B. V. Derjaguin, G. Sidorenkov, E. Zubashchenkov, and E. Kiseleva, Kinetic phenomena in boundary films of liquids, *Kolloidn. Zh.* **9**, 335 (1947).
- [43] A. Domínguez, D. Frydel, and M. Oettel, Multipole expansion of the electrostatic interaction between charged colloids at interfaces, *Phys. Rev. E* **77**, 020401(R) (2008).
- [44] R. Podgornik, General theory of charge regulation and surface differential capacitance, *J. Chem. Phys.* **149**, 104701 (2018).
- [45] A. Gupta, A. Govind Rajan, E. A. Carter, and H. A.

- Stone, Thermodynamics of electrical double layers with electrostatic correlations, *J. Phys. Chem. C* **124**, 26830 (2020).
- [46] See Supplemental Material at [URL link](#) for full details, which includes Refs. [61–63].
- [47] M. Teubner, Motion of charged colloidal particles, *J. Chem. Phys.* **76**, 5564 (1982).
- [48] A. Domínguez and M. Popescu, Force–dependence of the rigid–body motion for an arbitrarily shaped particle in a forced, incompressible Stokes flow, *Phys. Rev. Fluids*, in preparation (2024).
- [49] J. Happel and H. Brenner, *Low Reynolds Number Hydrodynamics* (Prentice-Hall, Englewood Cliffs, NJ, 1965).
- [50] S. Kim and S. J. Karrila, *Microhydrodynamics: Principles and Selected Applications* (Butterworth–Heinemann, New York, 1991).
- [51] This departs from the somewhat more usual approach of perturbing around the equilibrium state induced by a charged particle, which will be inhomogeneous. This is again a simplification which reduces the algebraic burden without sacrificing the physical picture.
- [52] Under the proviso that, irrespective of the nature of the ions, the addition of salts can be interpreted to affect only the value of  $c_0$ , and thus of  $\lambda_D$ .
- [53] This would correspond to, e.g., the lowest orders expansions for a typical Janus particle, for which the activity is due to an axisymmetric decoration by a catalyst of the surface of a homogeneous spherical core, so that activity and surface charge distributions are expected to be correlated.
- [54] Based on the values for  $\mathcal{A}$  and  $\sigma_s$  provided in Ref. [34] and  $q = e$ , we estimated  $|V^{(S)}/V^{(A)}| \approx 10^{-2}$  for a particle of radius  $R = 500$  nm.
- [55] Under the same proviso as in [52], this motility mechanism may consistently capture, as noted in Ref. [29], the qualitative features of the velocity dependence on  $\lambda_D/R$  observed in experiments with Pt-covered silica or polystyrene Janus spheres upon varying their size or adding small amounts of salts [32, 33, 56]. This provides an alternative to the models based on an electrokinetic current through the Pt film [21, 22, 32] or a very complex surface reaction [32, 56].
- [56] S. Ebbens, M.-H. Tu, J. R. Howse, and R. Golestanian, Size dependence of the propulsion velocity for catalytic Janus-sphere swimmers, *Phys. Rev. E* **85**, 020401(R) (2012).
- [57] M. J. Esplandiu, D. Reguera, and J. Fraxedas, Electrophoretic origin of long-range repulsion of colloids near water/Nafion interfaces, *Soft Matter* **16**, 3717 (2020).
- [58] M. J. Esplandiu, D. Reguera, D. Romero-Guzmán, A. M. Gallardo-Moreno, and J. Fraxedas, From radial to unidirectional water pumping in zeta-potential modulated Nafion nanostructures, *Nature Commun.* **13**, 2812 (2022).
- [59] R. Niu, P. Kreissl, A. T. Brown, G. Rempfer, D. Botin, C. Holm, T. Palberg, and J. de Graaf, Microfluidic pumping by micromolar salt concentrations, *Soft Matter* **13**, 1505 (2017).
- [60] R. Niu, A. Fischer, T. Palberg, and T. Speck, Dynamics of binary active clusters driven by ion-exchange particles, *ACS Nano* **12**, 10932 (2018).
- [61] M. Abramowitz and I. R. Stegun, (Eds.) *Handbook of mathematical functions* (Dover, New York, 1972).
- [62] I. S. Gradshteyn and I. M. Ryzhik, *Table of Integrals, Series, and Products*, 5th ed., edited by A. Jeffrey (Academic Press, London, 1994).
- [63] C. M. Bender and S. A. Orszag, *Advanced Mathematical Methods for Scientists and Engineers* (McGraw–Hill, 1978).

# Ionic self-phoresis maps onto correlation–induced self-phoresis

## Supplemental Material<sup>a</sup>

Alvaro Domínguez<sup>1,2,†</sup> and Mihail N. Popescu<sup>1,‡</sup>

<sup>1</sup>*Física Teórica, Universidad de Sevilla, Apdo. 1065, 41080 Sevilla, Spain*

<sup>2</sup>*Instituto Carlos I de Física Teórica y Computacional, 18071 Granada, Spain*

(Dated: April 26, 2024)

### I. HYDRODYNAMICS

The flow  $\mathbf{u}(\mathbf{r})$  is determined by the mechanical balance between the body force density acting on the solution, see Eq. (2),

$$\mathbf{f}(\mathbf{r}) = \mathbf{f}_+(\mathbf{r}) + \mathbf{f}_-(\mathbf{r}) = -c_+(\mathbf{r})\nabla\mu_+(\mathbf{r}) - c_-(\mathbf{r})\nabla\mu_-(\mathbf{r}), \quad (\text{I.1})$$

and the fluid stresses. This is expressed by the Stokes equation for incompressible flow,

$$\eta\nabla^2\mathbf{u} - \nabla p + \mathbf{f} = 0, \quad \nabla \cdot \mathbf{u} = 0, \quad (\text{I.2})$$

where  $\eta$  is the viscosity of the solution and  $p$  is the pressure field enforcing incompressibility. The hydrodynamic flow is subject to the boundary conditions of quiescent solution at infinity,

$$\mathbf{u}(|\mathbf{r}| \rightarrow \infty) \rightarrow 0, \quad (\text{I.3a})$$

which sets the rest frame with respect to which the velocities are measured, and of no slip at the surface of the particle, which translates with velocity  $\mathbf{V}$  and rotates with angular velocity  $\mathbf{\Omega}$ ,

$$\mathbf{u}(\mathbf{r}_p) = \mathbf{V} + \mathbf{\Omega} \times \mathbf{r}_p. \quad (\text{I.3b})$$

Finally, the yet unknown translational and rotational velocities  $\mathbf{V}$  and  $\mathbf{\Omega}$  of the overdamped motion of the particle are fixed by the requirement that the system “particle + fluid” does not experience external forces or torques.

### II. DETAILS OF THE CALCULATIONS IN THE QUASI-HOMOGENEOUS REGIME

The procedure is very similar to the one carried out in Ref. [1]. We start with the body force density (2), which, up to second–order in the small deviations from homogeneity, is given by

$$\mathbf{f}_\pm = -(c_0 + \delta c_\pm)\nabla(\mu_0 + \delta\mu_\pm) = -c_0\nabla\delta\mu_\pm - \delta c_\pm\nabla\delta\mu_\pm \quad (\text{II.1a})$$

$$\Rightarrow \mathbf{f} = -c_0\nabla(\delta\mu_+ + \delta\mu_-) - \delta c_+\nabla\delta\mu_+ - \delta c_-\nabla\delta\mu_-. \quad (\text{II.1b})$$

It is immediately apparent that, in the flow problem, it is necessary to go to the second order because at the first order,  $\mathbf{f}$  is a gradient, and thus cannot contribute to the fluid motion. But in the diffusion equations (1), the expansion of  $\mathbf{f}_\pm$  to first order is sufficient, and it leads to Laplace equations for the chemical potential deviations,

$$\nabla^2\delta\mu_\pm = 0, \quad (\text{II.2a})$$

with boundary conditions at the surface of the particle following from Eqs. (6b),

$$\mathbf{e}_r \cdot \nabla\delta\mu_\pm(\mathbf{r}_p) = -\frac{\mathcal{A}}{c_0\Gamma_\pm}\mathbb{A}(\mathbf{r}_p), \quad (\text{II.2b})$$

<sup>a</sup> Here, equations of the main text are referenced by their respective numbers. Equations appearing only in the Supplemental Material are cited by a combination of the section number (in Roman numerals) and the equation number within the section (in Arabic numerals).

<sup>†</sup> [dominguez@us.es](mailto:dominguez@us.es)

<sup>‡</sup> [mpopescu@us.es](mailto:mpopescu@us.es)

and at infinity, corresponding to the particle reservoir, see Eq. (6a),

$$\delta\mu_{\pm}(|\mathbf{r}| \rightarrow \infty) = 0. \quad (\text{II.2c})$$

Similarly, for the electrostatic problem the first order expansion is sufficient, and Eqs. (7, 8) render the boundary-value problem

$$\nabla^2\psi = -\frac{q}{\epsilon}(\delta c_+ - \delta c_-), \quad (\text{II.3a})$$

$$\mathbf{e}_r \cdot \nabla\psi(\mathbf{r}_p) = -\frac{\sigma_s}{\epsilon}\mathbb{S}(\mathbf{r}_p), \quad (\text{II.3b})$$

$$\psi(|\mathbf{r}| \rightarrow \infty) \rightarrow 0. \quad (\text{II.3c})$$

The ‘‘excess’’ concentrations  $\delta c_{\pm}$  follow from expanding at linear order the chemical potential (3) with the ideal gas approximation (Eq. (5)):

$$\delta\mu_{\pm} = \delta c_{\pm} \frac{\partial^2 h}{\partial c_{\pm}^2}(c_0, c_0) + \delta c_{\mp} \frac{\partial^2 h}{\partial c_+ \partial c_-}(c_0, c_0) \pm q\psi = \frac{1}{\beta c_0} \delta c_{\pm} \pm q\psi, \quad (\text{II.4})$$

which is Eq. (12). One notices immediately the relation

$$N(\mathbf{r}) := \delta c_+ + \delta c_- = \beta c_0(\delta\mu_+ + \delta\mu_-), \quad (\text{II.5})$$

for the deviations from homogeneity of the total concentration of ions. With  $\delta\mu_{\pm}(\mathbf{r})$  known as the solution of the boundary-value problem (II.2), the relations (II.4) provide  $\delta c_{\pm}(\mathbf{r})$ ; by plugging these into Eqs. (II.3) the boundary-value problem for the electric potential  $\psi(\mathbf{r})$  can be solved, and all the relevant functions are thus determined.

However, for the purpose of just calculating the phoretic velocities of the particle, not all of the above steps are necessary. As noticed, the first order terms in the expression (II.1a) for the force do not make contributions to the velocity. At the second order, we have

$$\begin{aligned} \mathbf{f} &= \mathbf{f}_+ + \mathbf{f}_- = -(\delta c_+ \nabla \delta\mu_+ + \delta c_- \nabla \delta\mu_-) = -\frac{1}{2}(\delta c_+ + \delta c_-) \nabla(\delta\mu_+ + \delta\mu_-) - \frac{1}{2}(\delta c_+ - \delta c_-) \nabla(\delta\mu_+ - \delta\mu_-) \\ &= -\frac{1}{4\beta c_0} \nabla(N^2) - \frac{1}{2} Q \nabla M, \end{aligned} \quad (\text{II.6})$$

after using the definitions (II.5, 14, 15). The first term in the final expression is a perfect gradient, and thus irrelevant for the motion of the particle; accordingly, after dropping it we arrive at the (for our purposes equivalent) expression (13) for the body force density responsible for the particle motility.

By subtracting the two problems contained in Eqs. (II.2) (one for  $\delta\mu_-$ , another one for  $\delta\mu_+$ ), one immediately obtains the boundary-value problem (18) obeyed by  $M(\mathbf{r})$ . Likewise, by subtracting the two Eqs. (II.4), one obtains the relation

$$2q\psi(\mathbf{r}) = M(\mathbf{r}) - \frac{1}{\beta c_0} Q(\mathbf{r}). \quad (\text{II.7})$$

And then, the electrostatic boundary-value problem (II.3), complemented by Eqs. (18), leads to the problem (19) for the charge concentration field. Due to the superposition of sources in Eq. (19b), one can write the solution as

$$Q(\mathbf{r}) = Q^{(\text{A})}(\mathbf{r}) + Q^{(\text{S})}(\mathbf{r}), \quad (\text{II.8})$$

where each field satisfies a different problem:

$$\nabla^2 Q^{(\text{A})}(\mathbf{r}) = \frac{1}{\lambda_D^2} Q^{(\text{A})}(\mathbf{r}), \quad (\text{II.9a})$$

$$\mathbf{e}_r \cdot \nabla Q^{(\text{A})}(\mathbf{r}_p) = -\frac{\mathcal{A}}{\Delta} \mathbb{A}(\mathbf{r}_p), \quad (\text{II.9b})$$

$$Q^{(\text{A})}(|\mathbf{r}| \rightarrow \infty) = 0, \quad (\text{II.9c})$$

and

$$\nabla^2 Q^{(\mathbb{S})}(\mathbf{r}) = \frac{1}{\lambda_D^2} Q^{(\mathbb{S})}(\mathbf{r}), \quad (\text{II.10a})$$

$$\mathbf{e}_r \cdot \nabla Q^{(\mathbb{S})}(\mathbf{r}_p) = \frac{\sigma_s}{q\lambda_D^2} \mathbb{S}(\mathbf{r}_p), \quad (\text{II.10b})$$

$$Q^{(\mathbb{S})}(|\mathbf{r}| \rightarrow \infty) = 0, \quad (\text{II.10c})$$

respectively.

### III. MAPPING BETWEEN IONIC SELF-PHORESIS AND CICP

The relevant ingredients of the model introduced in Ref. [1] for CICP are the concentration field  $n(\mathbf{r})$  of a chemical, its chemical potential  $\mu(\mathbf{r})$  and the associated free energy,

$$\mathcal{H}_{\text{CICP}}[n] = \int_{\text{fluid}} d^3\mathbf{r} \left[ h(n) + \frac{1}{2} \lambda^2 |\nabla n|^2 \right], \quad (\text{III.1})$$

where  $\lambda$  is a parameter related to the correlation length (see Eq. (III.2)). Notice that, unlike with the free energy employed in Eq. (4), the correlations are modeled through a square-gradient term in the concentration without the mediation of a field like the electric potential  $\psi(\mathbf{r})$ . The quasi-homogeneous approximation is obtained by linearizing around the equilibrium state  $n(\mathbf{r}) = n_0$ , in which the correlation length is given as

$$\xi = \frac{\lambda}{\sqrt{h''(n_0)}}. \quad (\text{III.2})$$

The following table provides, in a side-by-side form, the mapping between this model for CICP and the model presented in the main text for ionic chemophoresis.

eq. numbers in this work	ionic chemophoresis	correlation-induced chemophoresis (CICP)	eq. numbers in Suppl. Mat. [1]
(13)	$\mathbf{f} = -\frac{1}{2} Q \nabla M$	$\mathbf{f} = -n_0 \Psi \nabla \mu$	(III.31)
(18a)	$\nabla^2 M = 0$	$\nabla^2 \mu = 0$	(II.5)
(18b)	$\mathbf{e}_r \cdot \nabla M(R\mathbf{e}_r) = -\frac{\mathcal{A}}{\beta c_0 \Delta} \mathbb{A}(\mathbf{e}_r)$	$\mathbf{e}_r \cdot \nabla \mu(R\mathbf{e}_r) = -\underbrace{\frac{q}{n_0 \Gamma}}_{b_1} \mathbb{A}(\mathbf{e}_r)$	(II.6)
(18c)	$M(\mathbf{r} \rightarrow \infty) = 0$	$\mu(\mathbf{r} \rightarrow \infty) = \mu_0$	(II.6)
(II.9a, II.10a)	$\nabla^2 Q^{(\mathbb{A}, \mathbb{S})} = \lambda_D^{-2} Q^{(\mathbb{A}, \mathbb{S})}$	$\nabla^2 \Psi = \xi^{-2} \Psi$	(II.10)
(II.9b)	$\left. \begin{aligned} \mathbf{e}_r \cdot \nabla Q^{(\mathbb{A})}(R\mathbf{e}_r) &= -\frac{\mathcal{A}}{\Delta} \mathbb{A}(\mathbf{e}_r) \\ \mathbf{e}_r \cdot \nabla Q^{(\mathbb{S})}(R\mathbf{e}_r) &= \frac{\sigma_s}{q\lambda_D^2} \mathbb{S}(\mathbf{e}_r) \end{aligned} \right\}$	$\mathbf{e}_r \cdot \nabla \Psi(R\mathbf{e}_r) = \underbrace{\frac{q}{n_0^2 \Gamma} \left( \frac{\xi}{\lambda} \right)^2}_{b_2} \mathbb{A}(\mathbf{e}_r)$	(II.12)
(II.10a)			
(II.9c, II.10c)	$Q^{(\mathbb{A}, \mathbb{S})}(\mathbf{r} \rightarrow \infty) = 0$	$\Psi(\mathbf{r} \rightarrow \infty) = 0$	(II.11)

This table leads to the following “translation rules”:

ionic chemophoresis	$M$	$Q^{(\mathbb{A})}$	$Q^{(\mathbb{S})}$	$\lambda_D$	$\mathcal{A}/\beta c_0 \Delta$	$-\mathcal{A}/\Delta$	$\sigma_s/q\lambda_D^2$	$\mathbb{A} = \sum_{\ell m} a_{\ell m} Y_{\ell m}$	$\mathbb{S} = \sum_{\ell m} s_{\ell m} Y_{\ell m}$
<b>CICP</b>	$\mu - \mu_0$	$2n_0\Psi$		$\xi$	$b_1$	$2b_2n_0$		$\mathbb{A} = \sum_{\ell m} a_{\ell m} Y_{\ell m}$	

The phoretic velocities for CICP can be represented with the same kind of sums over modes as in Eqs. (21) (see Eqs. (III.37, III.44) in Ref. [1])

$$\mathbf{V} = V_0 \sum_{\ell m, \ell' m'} a_{\ell m} a_{\ell' m'} \cdots, \quad \mathbf{\Omega} = \Omega_0 \sum_{\ell m, \ell' m'} a_{\ell m} a_{\ell' m'} \cdots, \quad (\text{III.3})$$

with the characteristic scales (see Eqs. (III.38, II.2))

$$V_0 = b_1 b_2 n_0 \frac{R^3}{6\pi\eta} \left(\frac{R}{\xi}\right)^2, \quad \Omega_0 = \frac{3V_0}{4R}. \quad (\text{III.4})$$

Therefore, making use of the translation table one arrives at the expansions (21a, 21b) with the scales shown in Eq. (21c):

$$V^{(\mathbb{A})} \longleftrightarrow -V_0 = -\frac{\mathcal{A}}{\beta c_0 \Delta} \left(-\frac{\mathcal{A}}{2\Delta}\right) \frac{R^3}{6\pi\eta} \left(\frac{R}{\lambda_D}\right)^2 = \frac{q^2 R^5 \mathcal{A}^2}{6\pi\eta\epsilon\Delta^2}, \quad (\text{III.5a})$$

$$V^{(\mathbb{S})} \longleftrightarrow \left(\frac{R}{\lambda_D}\right)^{-2} V_0 = \left(\frac{R}{\lambda_D}\right)^{-2} \frac{\mathcal{A}}{\beta c_0 \Delta} \frac{\sigma_s}{2q\lambda_D^2} \frac{R^3}{6\pi\eta} \left(\frac{R}{\lambda_D}\right)^2 = \frac{qR^3 \mathcal{A} \sigma_s}{6\pi\eta\epsilon\Delta}. \quad (\text{III.5b})$$

#### IV. THE PHORETIC VELOCITIES

The expressions (21) follow from solving the boundary-value problems (18, 19) as expansions in spherical harmonics (see Eq. (20)), and evaluating the integrals appearing in Eqs. (9) with Eqs. (11) for the hydrodynamic kernels and Eq. (13) for the force density. The details can be found in Ref. [1] and lead to explicit expressions for the  $g$  functions and the  $\mathbf{G}$  vectors. Specifically, one has (we here use the short-hand notations  $\lambda \equiv \lambda_D/R$ ,  $s \equiv r/R$ )

$$g_{\ell\ell'}^{\perp}(\lambda) := \int_1^{\infty} ds \left(-\frac{1}{2s^3} + \frac{3}{2s} - 1\right) s^{-\ell'} c_{\ell}(s, \lambda), \quad (\text{IV.1a})$$

$$g_{\ell\ell'}^{\parallel}(\lambda) := \int_1^{\infty} ds \left(\frac{1}{4s^3} + \frac{3}{4s} - 1\right) s^{-\ell'} c_{\ell}(s, \lambda), \quad (\text{IV.1b})$$

and

$$g_{\ell\ell'}^{\tau}(\lambda) := \int_1^{\infty} ds \left(\frac{1}{s^3} - 1\right) s^{1-\ell'} c_{\ell}(s, \lambda). \quad (\text{IV.1c})$$

One can recognize the pieces stemming from the hydrodynamic kernels (11), while the functions

$$c_{\ell}(s, \lambda) := \gamma_{\ell}(\lambda) \frac{K_{\ell+1/2}(s/\lambda)}{\sqrt{s}}, \quad (\text{IV.2})$$

are the coefficients in the expansion in spherical harmonics of the solution to Eqs. (19); the functions  $K_n(x)$  are the modified Bessel functions of the second kind of order  $n$  [2, 3], and

$$\gamma_{\ell}(\lambda) = -\frac{\lambda^2}{(\ell+1)K_{\ell+1/2}(\lambda^{-1}) + \lambda^{-1}K_{\ell-1/2}(\lambda^{-1})}. \quad (\text{IV.3})$$

And one also has the vectors

$$\begin{aligned} \mathbf{G}_{\ell m; \ell' m'}^\perp &= \sqrt{(2\ell+1)(2\ell'+1)} \begin{pmatrix} 1 & \ell & \ell' \\ 0 & 0 & 0 \end{pmatrix} \\ &\times \left[ \mathbf{e}_z \begin{pmatrix} 1 & \ell & \ell' \\ 0 & m & m' \end{pmatrix} - \frac{\mathbf{e}_x - i\mathbf{e}_y}{\sqrt{2}} \begin{pmatrix} 1 & \ell & \ell' \\ 1 & m & m' \end{pmatrix} + \frac{\mathbf{e}_x + i\mathbf{e}_y}{\sqrt{2}} \begin{pmatrix} 1 & \ell & \ell' \\ -1 & m & m' \end{pmatrix} \right], \end{aligned} \quad (\text{IV.4a})$$

$$\begin{aligned} \mathbf{G}_{\ell m; \ell' m'}^\parallel &= -\frac{\sqrt{(2\ell+1)(2\ell'+1)}}{\ell'+1} \begin{pmatrix} 1 & \ell & \ell' \\ 0 & 0 & 0 \end{pmatrix} \\ &\times \left\{ m' \left[ \frac{\mathbf{e}_x + i\mathbf{e}_y}{\sqrt{2}} \begin{pmatrix} 1 & \ell & \ell' \\ -1 & m & m' \end{pmatrix} + \frac{\mathbf{e}_x - i\mathbf{e}_y}{\sqrt{2}} \begin{pmatrix} 1 & \ell & \ell' \\ 1 & m & m' \end{pmatrix} \right] \right. \\ &+ \frac{\sqrt{\ell'(\ell'+1) - m'(m'+1)}}{\sqrt{2}} \left[ \frac{\mathbf{e}_x - i\mathbf{e}_y}{\sqrt{2}} \begin{pmatrix} 1 & \ell & \ell' \\ 0 & m & m'+1 \end{pmatrix} - \mathbf{e}_z \begin{pmatrix} 1 & \ell & \ell' \\ -1 & m & m'+1 \end{pmatrix} \right] \\ &\left. + \frac{\sqrt{\ell'(\ell'+1) - m'(m'-1)}}{\sqrt{2}} \left[ -\frac{\mathbf{e}_x + i\mathbf{e}_y}{\sqrt{2}} \begin{pmatrix} 1 & \ell & \ell' \\ 0 & m & m'-1 \end{pmatrix} - \mathbf{e}_z \begin{pmatrix} 1 & \ell & \ell' \\ 1 & m & m'-1 \end{pmatrix} \right] \right\}, \end{aligned} \quad (\text{IV.4b})$$

$$\mathbf{G}_{\ell m; \ell' m'}^\tau = -\frac{i(-1)^m}{\ell+1} \delta_{\ell, \ell'} \left[ \mathbf{e}_z m' \delta_{m+m', 0} + \sqrt{\ell(\ell+1) + m m'} \left( \frac{\mathbf{e}_x - i\mathbf{e}_y}{2} \delta_{m+m', -1} + \frac{\mathbf{e}_x + i\mathbf{e}_y}{2} \delta_{m+m', 1} \right) \right], \quad (\text{IV.4c})$$

expressed in a Cartesian basis  $\{\mathbf{e}_x, \mathbf{e}_y, \mathbf{e}_z\}$  and in terms of the Wigner 3j symbols.

#### A. Limiting behaviors in $\lambda = \lambda_D/R$

The integrals appearing in the definitions of the  $g$ -functions can be expressed analytically in terms of the exponential integral function [1], and not all of them are needed: because of the selection rules (22), the only functions that are required are of the form

$$g_{\ell, |\ell \pm 1|}^\perp, g_{|\ell \pm 1|, \ell}^\perp, g_{\ell, |\ell \pm 1|}^\parallel, g_{|\ell \pm 1|, \ell}^\parallel, g_{\ell, \ell \neq 0, 0}^\tau. \quad (\text{IV.5})$$

The plots in Fig. S1 show some of them. Of particular interest are the limiting behaviors, already explored in Ref. [1]. When  $\lambda \rightarrow 0$ , the functions (IV.2) behave exponentially,

$$c_\ell(s, \lambda) \approx -\frac{\lambda^3}{s} e^{(1-s)/\lambda}. \quad (\text{IV.6})$$

Therefore, the integrals in the definitions (IV.1) of the  $g$ -functions are exponentially dominated by the lower limit ( $s = 1$ ) and can be thus approximated using Watson's lemma (see, e.g., [4]) in order to obtain the leading asymptotic behavior,

$$g_{\ell\ell'}^\perp \approx 3\lambda^6, \quad g_{\ell\ell'}^\parallel \approx \frac{3}{2}\lambda^5, \quad g_{\ell\ell'}^\tau \approx 3\lambda^5, \quad (\text{IV.7})$$

(this is Eq. (23)), which turns out to be independent of the value of the indices  $\ell, \ell'$ .

In the opposite limit,  $\lambda \rightarrow \infty$ , one has to address separately the contributions associated to  $V^{(\text{A})}$  and  $V^{(\text{S})}$ , i.e., following from the decomposition (II.8). One first notices that the functions (IV.2) behave in this limit as

$$c_\ell(s, \lambda) \approx -\frac{\lambda^2}{(\ell+1)s^{\ell+1}}, \quad (\text{IV.8})$$

and all the integrals that comply with the constraints (IV.5) are convergent. Thus, all the  $g$ -functions scale as  $\lambda^2$  in this limit. Since the velocity scales  $V^{(\text{S})}$  and  $\Omega^{(\text{S})}$  are always accompanied by a factor  $\lambda^{-2} = (R/\lambda_D)^2$  in expressions (21), this gives a  $\lambda$ -independent value for the phoretic velocity stemming from the surface-charge-driven mechanism.

One would be tempted to conclude that the velocity due to the correlation-driven mechanism will therefore grow as  $\lambda^2$ . This is however not the case because the leading asymptotic contributions cancel altogether when inserted in

the expressions (21). This can be easily understood as follows: if the limit  $\lambda_D = R\lambda \rightarrow \infty$  is taken in Eq. (II.9a), the boundary-value problem for the field  $Q^{(\text{A})}(\mathbf{r})$  becomes the same as the problem (18) for the field  $M(\mathbf{r})$ , and one can write  $Q^{(\text{A})} = M/\beta c_0$ , so that the contribution to the force field (II.6) is a perfect gradient, and thus irrelevant. This means that this contribution to the phoretic velocity is determined by the next-to-leading asymptotic behavior of the  $g$  functions. This was done explicitly in Sec. VI of the Supplementary Material of Ref. [1] for the functions  $g^\perp, g^\parallel$ ; the same method can be applied straightforwardly to  $g^\tau$ . The final conclusion is that also this piece of the velocity acquires a finite,  $\lambda$ -independent value in this limit.

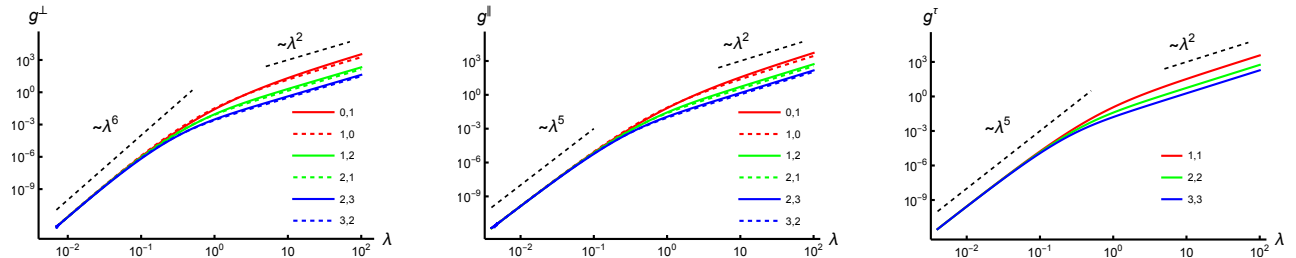


FIG. S1. Log-log plots of the functions  $g_{\ell\ell'}^\perp(\lambda), g_{\ell\ell'}^\parallel(\lambda), g_{\ell\ell'}^\tau(\lambda)$  for some choices of the pairs  $(\ell, \ell')$  (as indicated by the labels) that fulfill the constraints (IV.5). Also shown are the asymptotic behaviors derived analytically.

- 
- [1] A. Domínguez, M. N. Popescu, C. M. Rohwer, and S. Dietrich, Self-motility of an active particle induced by correlations in the surrounding solution, *Phys. Rev. Lett.* **125**, 268002 (2020).
  - [2] M. Abramowitz and I. R. Stegun, (Eds.) *Handbook of mathematical functions* (Dover, New York, 1972).
  - [3] I. S. Gradshteyn and I. M. Ryzhik, *Table of Integrals, Series, and Products*, 5th ed., edited by A. Jeffrey (Academic Press, London, 1994).
  - [4] C. M. Bender and S. A. Orszag, *Advanced Mathematical Methods for Scientists and Engineers* (McGraw-Hill, 1978).